VASP is a CXCR2-interacting protein that regulates CXCR2-mediated polarization and chemotaxis

Nicole F. Neel[1,2], Melanie Barzik[5], Dayanidhi Raman[1,2], Tammy Sobolik-Delmaire[1,2], Jiqing Sai[1,2], Amy J. Ham[3,4], Raymond L. Mernaugh[3], Frank B. Gertler[5] and Ann Richmond[1,2,*]

[1]Department of Veterans Affairs, Nashville, TN 37212, USA
[2]Department of Cancer Biology, [3]Department of Biochemistry and [4]Mass Spectrometry Research Center, Vanderbilt University School of Medicine, Nashville, TN 37232, USA
[5]Department of Biology, Massachusetts Institute of Technology, Cambridge, MA 02139, USA
*Author for correspondence (e-mail: ann.richmond@vanderbilt.edu)

Accepted 24 February 2009
Journal of Cell Science 122, 1882-1894 Published by The Company of Biologists 2009
doi:10.1242/jcs.039057

Summary

Chemotaxis regulates the recruitment of leukocytes, which is integral for a number of biological processes and is mediated through the interaction of chemokines with seven transmembrane G-protein-coupled receptors. Several studies have indicated that chemotactic signaling pathways might be activated via G-protein-independent mechanisms, perhaps through novel receptor-interacting proteins. CXCR2 is a major chemokine receptor expressed on neutrophils. We used a proteomics approach to identify unique ligand-dependent CXCR2-interacting proteins in differentiated neutrophil-like HL-60 cells. Using this approach, vasodilator-stimulated phosphoprotein (VASP) was identified as a CXCR2-interacting protein. The interaction between CXCR2 and VASP is direct and enhanced by CXCL8 stimulation, which triggers VASP phosphorylation via PKA- and PKCδ-mediated pathways. The interaction between CXCR2 and VASP requires free F-actin barbed ends to recruit VASP to the leading edge. Finally, knockdown of VASP in HL-60 cells results in severely impaired CXCR2-mediated chemotaxis and polarization. These data provide the first demonstration that direct interaction of VASP with CXCR2 is essential for proper CXCR2 function and demonstrate a crucial role for VASP in mediating chemotaxis in leukocytes.

Supplementary material available online at
http://jcs.biologists.org/cgi/content/full/122/11/1882/DC1

Key words: CXCR2, VASP, Chemotaxis, Actin, Phosphorylation

Introduction

CXCR2 is a chemokine receptor implicated in the recruitment of leukocytes from the bloodstream during inflammation. CXCR2-mediated chemotaxis is completely inhibited by treatment with pertussis toxin, indicating that CXCR2 is a Gαi-coupled receptor (Jones et al., 1995; Neptune et al., 1999). The signaling pathways activated as a result of the uncoupling of the Gβγ subunit from the heterotrimeric complex include phospholipase Cβ, phosphatidylinositol-3-kinase, and mitogen-activated proteins. Additional signaling pathways that mediate the chemotactic response might be activated through novel receptor-interacting proteins (Luttrell et al., 1999; Richardson et al., 1998; Tilton et al., 2000). Of particular interest are the proteins that initiate and propagate the chemotactic response once a chemokine binds its receptor. To identify protein complexes that associate with CXCR2, we utilized the C-terminal domain of CXCR2 in a yeast two-hybrid analysis to identify a number of CXCR2-interacting proteins (unpublished data) (Fan et al., 2001a; Fan et al., 2001b; Fan et al., 2002). However, this approach does not permit identification of receptor-protein complexes that bind other intracellular domains or that are induced by ligand stimulation.

The current study describes the identification of a ligand-mediated receptor-protein interaction from differentiated HL-60 cells (dHL-60) using immunoprecipitation followed by proteomics analysis. Here, we identify vasodilator-stimulated phosphoprotein (VASP) as a novel CXCR2-interacting protein. VASP is a member of the Ena/VASP family of proteins that regulate the geometry of assembling actin networks (Krause et al., 2003). Ena/VASP proteins localize to sites of active actin remodeling, such as filopodia, lamellipodia and focal adhesions (Gertler et al., 1996; Lanier et al., 1999; Reinhard et al., 1992). Localization of VASP at the fast-growing barbed ends of actin promotes filament elongation by recruiting profilin-actin complexes and antagonizing capping proteins (Barzik et al., 2005; Ferron et al., 2007; Pasic et al., 2008). In addition, VASP reduces branching of F-actin through an unknown mechanism (Bear et al., 2002; Skoble et al., 2001). VASP contains two conserved EVH (Ena/VASP homology domains, EVH1 and EVH2) that flank a central proline-rich region and a number of conserved serine/threonine residues that can be phosphorylated by PKA, PKC and PKG (Butt et al., 1994; Chitaley et al., 2004; Eigenthaler et al., 1992; Gertler et al., 1996; Lambrechts et al., 2000).

Phosphorylation of Ena/VASP proteins at the conserved N-terminal serine (Ser157) leads to a major conformational change, which results in an electrophoretic mobility shift and alterations in protein-protein interactions (Gertler et al., 1996; Halbrugge et al., 1990; Lambrechts et al., 2000). Interestingly, PKCδ negatively regulates VASP-dependent filopodia formation in collagen-activated platelets and reduces phosphorylation at Ser157 through an unknown mechanism (Pula et al., 2006). VASP contains two other phosphorylation sites: Ser239 and Thr278 (Butt et al., 1994). The equivalents of Ser157 and Ser239 but not Thr278 are found in Mena, whereas Ser157 is the only site found in EVL (Gertler et al., 1996). In vitro, VASP phosphorylation at Ser239 or Thr278 decreases its anti-capping and filament-bundling activity, and its ability to bind F- and G-actin (Barzik et al., 2005; Harbeck et al., 2000). Although

Thr278 can be minimally phosphorylated in vitro by PKA and PKG, recent studies identified Thr278 as a substrate for AMP-activated protein kinase (AMPK) (Blume et al., 2007). In cells, phosphorylation at Thr278 is associated with decreased F-actin content, suggesting that it has a negative role in F-actin assembly (Blume et al., 2007), whereas phosphorylation at Ser239 in response to nitric oxide (NO) treatment disrupts VASP localization in lamellipodia (Lindsay et al., 2007) and is associated with loss of lamellipodial protrusions. By contrast, phosphorylation at Ser157 (or of the equivalent residue in Mena) does not affect interaction with actin, but is correlated with activities such as driving filopodia formation (Applewhite et al., 2007; Barzik et al., 2005; Loureiro et al., 2002) and regulation of protein-protein interactions, such as those of spectrin α (Benz et al., 2008). It is clear that differential phosphorylation of VASP at each of the residues modulates its function.

Ena/VASP proteins regulate cell motility in a variety of cell types but the specific role might be cell-type specific and vary depending on experimental conditions (Wills et al., 1999; Bashaw et al., 2000; Bear et al., 2000; Garcia Arguinzonis et al., 2002; Menzies et al., 2004; Kwiatkowski et al., 2007). Studies using *Dictyostelium* dsvasp-null cells revealed defects in persistent chemotaxis in response to the cAMP chemoattractant, suggesting a role for VASP in gradient sensing (Han et al., 2002), but its role in persistent directional migration in mammalian cells has not been extensively investigated. Specifically, its involvement in CXCR2-mediated neutrophil chemotaxis remains undefined.

We demonstrate here that VASP is phosphorylated upon CXCL8 stimulation on Ser157, Ser239 and Thr278. The Ser239 and Thr278 phosphorylations of the EVH2 domain modulate its interaction with CXCR2. Moreover, depletion of VASP in CXCR2-expressing dHL-60 cells specifically diminishes CXCR2-mediated chemotaxis, demonstrating the important functional significance for the CXCR2-VASP interaction.

Results

VASP is a CXCR2-interacting protein

A proteomics approach was used to identify novel ligand-independent and ligand-dependent CXCR2-interacting proteins. dHL-60 cells stably overexpressing human CXCR2 were stimulated with vehicle or CXCL8 for 1 minute. CXCR2 was immunoprecipitated with associating proteins from lysates of these cells using N-terminally targeted CXCR2 rabbit polyclonal antibodies, or control normal rabbit IgG coupled to Sepharose beads. Eluted proteins were digested with trypsin and the tryptic peptides were subjected to tandem liquid chromatography-mass spectrometry (LC-MS/MS) analysis. Spectra from tryptic peptides were compared with known spectra using the Sequest algorithms to identify proteins. Proteins identified from control rabbit IgG samples were subtracted from CXCR2 antibody samples. This analysis was repeated four times and proteins consistently identified were validated by immunoprecipitation assay.

VASP was consistently identified in CXCR2-immunoprecipitated samples from CXCL8-stimulated cells. Neither of the two closely related Ena/VASP family members (EVL and Mena) was identified in the proteomic studies. Interaction of VASP with CXCR2 in dHL-60 cells was confirmed by immunoprecipitation and western blot analysis in untreated cells and cells stimulated with CXCL8 (Fig. 1A). Interestingly, VASP is phosphorylated upon CXCL8 stimulation, indicated by the electrophoretic mobility shift (which is largely due to phosphorylation at Ser157) (Butt et al., 1994), and there is an increase in the amount of phosphorylated VASP that coimmunoprecipitates with CXCR2, as quantified by the amount of the shifted band present in immunoprecipitate eluates normalized to the total amount of VASP (Fig. 1B). To verify that CXCR2 coimmunoprecipitates with phosphorylated VASP, we analyzed CXCR2 immunoprecipitates by western blot using Ser157-*P*, Ser239-*P* and Thr278-*P* VASP-specific antibodies. As shown in Fig. 1C, VASP phosphorylated on Ser157, Ser239 and Ser278 is present

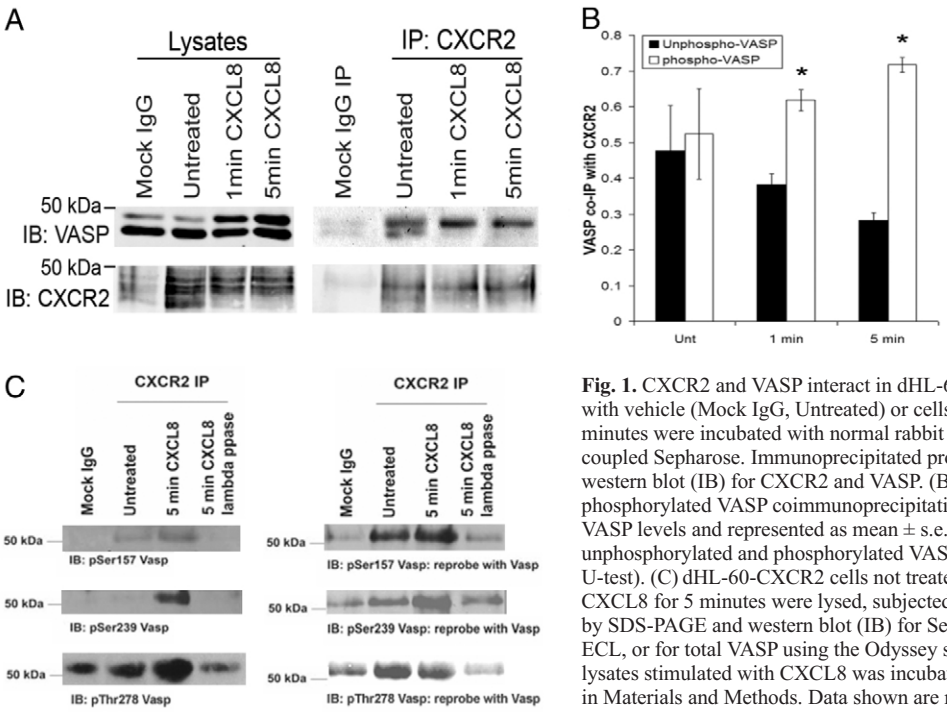

Fig. 1. CXCR2 and VASP interact in dHL-60-CXCR2 cells. (A) Lysates from cells stimulated with vehicle (Mock IgG, Untreated) or cells stimulated with 100 ng/ml CXCL8 for 1 or 5 minutes were incubated with normal rabbit IgG- (Mock IgG) or rabbit anti-CXCR2 antibody-coupled Sepharose. Immunoprecipitated proteins were eluted and analyzed by SDS-PAGE and western blot (IB) for CXCR2 and VASP. (B) Quantification of unphosphorylated and Ser157-phosphorylated VASP coimmunoprecipitating with CXCR2. Values are normalized to total VASP levels and represented as mean ± s.e.m. Significant differences between the unphosphorylated and phosphorylated VASP in the IP are indicated (*$P \leq 0.05$, Mann Whitney U-test). (C) dHL-60-CXCR2 cells not treated (lane 2) or treated (lane 3) with 100 ng/ml CXCL8 for 5 minutes were lysed, subjected to immunoprecipitation as above, and analyzed by SDS-PAGE and western blot (IB) for Ser157-*P*, Ser239-*P* or P-Thr278-*P* VASP using ECL, or for total VASP using the Odyssey system or ECL. One set of immunoprecipitated lysates stimulated with CXCL8 was incubated with lambda phosphatase (lane 4) as described in Materials and Methods. Data shown are representative of three separate experiments.

in CXCR2 immunoprecipitates. In some experiments where the gel was run for a longer period, we observed that CXCR2 immunoprecipitated VASP migrates more slowly than VASP in cell lysates. To determine whether the VASP-CXCR2 interaction was phosphorylation dependent, HL60 cells were stimulated with CXCL8 for 5 minutes and immunoprecipitated with CXCR2 antibody. One aliquot of immunoprecipitate from stimulated cells received lambda phosphatase buffer only (Fig. 1C, lane 3), whereas the other received lambda phosphatase (Fig. 1C, lane 4) before washing the beads and subjecting the eluates to electrophoresis. As shown in Fig. 1C, phosphatase treatment dramatically decreased the association of CXCR2 with VASP as detected by total VASP or Ser157-*P*, Ser239-*P* or Thr278-*P*. Densitometric quantification of the amount of phosphorylated VASP associated with receptor shows only a modest increase in Ser157-*P* VASP and a 2.75-fold increase in Ser239-*P* VASP in the CXCR2 immunoprecipitate after 5 minutes of ligand stimulation. In addition, there is a two- to threefold increase in the total amount of VASP associated with the receptor 5 minutes after ligand stimulation. There is clearly some basal association of VASP with the receptor before ligand activation, based upon the immunoprecipitation and western blot results, but the amount of Ser157-*P* VASP and Ser239-*P* associated with the receptor is much less before ligand activation. Since HL-60 cells produce CXCL8, this low level of basally phosphorylated VASP associated with CXCR2 is probably due to an autocrine activation of the receptor. Addition of ligand stimulates the amount of phosphorylated Ser157, Ser239 and Thr278 VASP that immunoprecipitates with the receptor. However, it is also possible that the basal unphosphorylated VASP in the CXCR2 immunoprecipitations is not due to a direct binding of VASP to

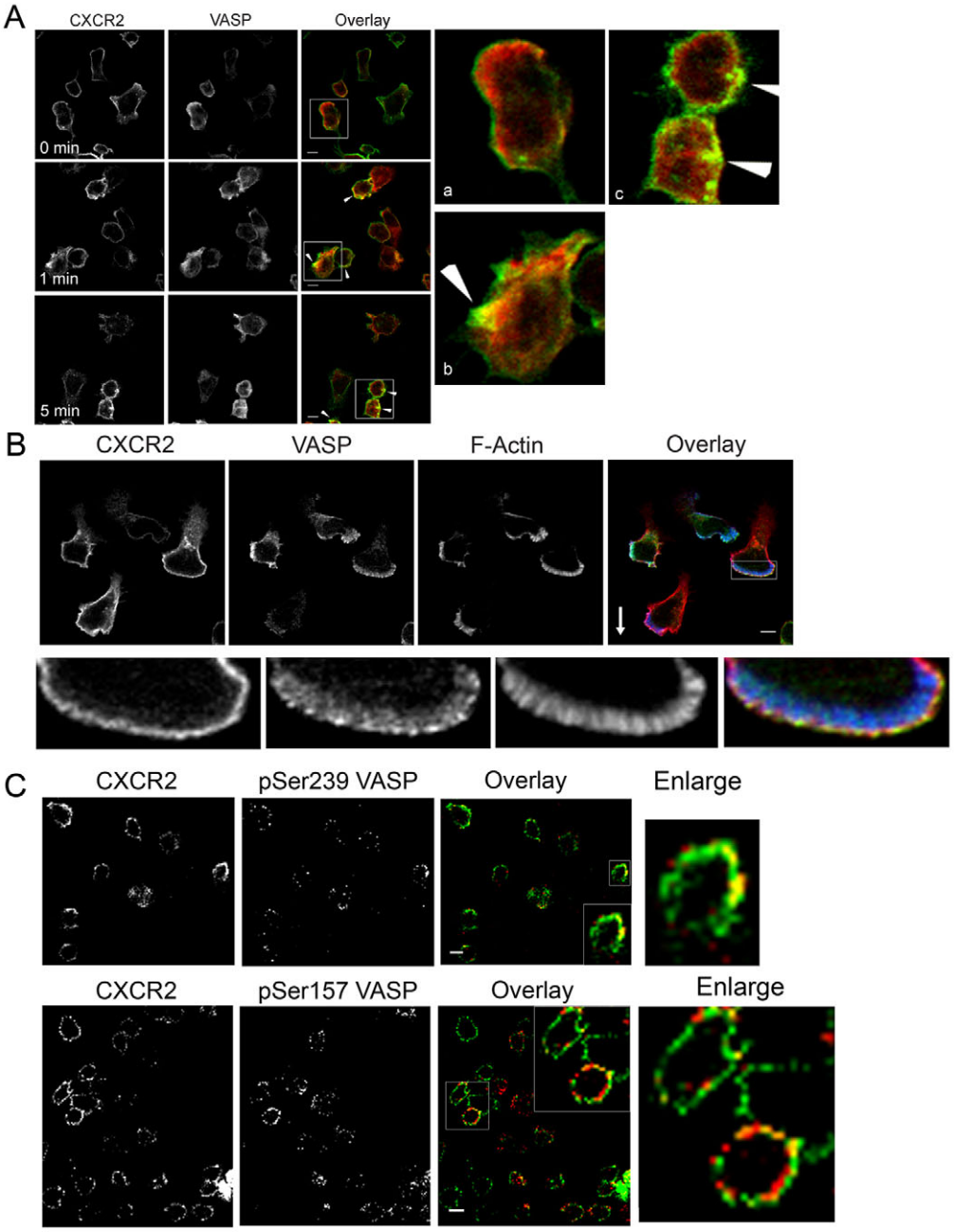

Fig. 2. CXCR2 and VASP localize to plasma membrane ruffles upon global and directional CXCL8 stimulation.
(A) Immunofluorescence confocal images of CXCR2 and VASP staining in dHL-60-CXCR2 cells stimulated globally with vehicle (0 minutes) or 100 ng/ml of CXCL8 for 1 or 5 minutes. Colocalization after both 1 and 5 minutes of stimulation is indicated by arrows. Images represent single *z*-sections of 0.38 μm. Overlay images are pseudocolored where green is CXCR2 and red is VASP. Images after 0 minutes (a), 1 minute (b), and 5 minutes (c) stimulation are enlarged ×5 from the boxed areas on the left.
(B) Immunofluorescence confocal images of CXCR2, VASP and F-actin staining in dHL-60-CXCR2 cells stimulated directionally with 50 ng/ml CXCL8 in a Zigmond chamber for 15 minutes. The arrow indicates the direction of CXCL8 gradient (0-50 ng/ml CXCL8). Image represents a single *z*-section of 0.35 μm pseudocolored, where green is VASP, red is CXCR2, and blue is F-actin.
(C) Immunofluorescence confocal images of CXCR2 and VASP phosphorylated on Ser157 (pPSer157 VASP) or Ser239 (pSer239) following 1 minute of global CXCL8 (100 ng/ml) stimulation. Overlay images are pseudocolored, where green is CXCR2 and red is pVASP. Image represents a single *z*-section of 0.28 μm. Insets are enlarged ×2 from boxed areas in originals. Images were processed using AdobePhotoshop. Scale bars: 5 μm. Data shown are representative of three separate experiments.

CXCR2, but could be the result of association of VASP with actin, which comes down in the immunoprecipitate.

To determine whether CXCR2 and VASP colocalize upon CXCL8 stimulation, we performed immunofluorescence staining and confocal imaging on cells stimulated with CXCL8 globally and directionally. As shown in Fig. 2A, VASP primarily localized to the cytoplasm with minimal plasma membrane localization seen in vehicle-stimulated cells. However, upon global stimulation with CXCL8 for 1 or 5 minutes, both VASP and CXCR2 localized to membrane ruffles. In addition, CXCR2 and VASP localized to the tips of F-actin-rich lamellipodia at the leading edge of the dHL-60 cells that were directionally stimulated with CXCL8 (Fig. 2B). VASP exhibited a punctate staining pattern in the lamellipodia with the most concentrated regions colocalizing with CXCR2 at the tips of actin bundles (indicated by the yellow color in the overlay of Fig. 2A,B). These data identify VASP as a CXCR2-interacting protein that localizes with CXCR2 in the membrane of cells stimulated with a CXCL8 gradient. The punctate areas of VASP colocalization with CXCR2 suggested that only a portion of the total VASP in the cells interacts with CXCR2. Some of the VASP not associated with CXCR2 at the leading edge appeared to be associated with actin as indicated by the magenta color in Fig. 2B, whereas the VASP-CXCR2 association is indicated by yellow color in the overlay. These data are consistent with immunoprecipitation data, indicating a basal coimmunoprecipitation of VASP and CXCR2, but an increased amount of phosphorylated VASP interacting with CXCR2 upon ligand stimulation. Therefore, localization of phosphorylated VASP using specific antibodies to Ser157-*P* and Ser239-*P* was examined. As expected, VASP phosphorylated on Ser239 strongly colocalized with CXCR2 and F-actin in cells stimulated with CXCL8 (Fig. 2C). VASP phosphorylated on Ser157 also showed some colocalization with CXCR2 (Fig. 2C). This is in agreement with the coimmunoprecipitation and western blot data shown in Fig. 1C. In sum, these data demonstrate that phosphorylated VASP interacts with CXCR2 at the plasma membrane upon CXCL8 stimulation.

CXCR2 directly interacts with VASP

Since VASP interacts with a number of proteins, we investigated whether the interaction between CXCR2 and VASP is direct or occurs indirectly through an additional protein. Purified regions of GST-CXCR2 C-terminus (residues 311-330 or 331-355) and full-length His-tagged VASP were used in binding assays. Purified His-VASP interacted in a concentration-dependent manner with residues 331-355 from the C-terminus of CXCR2 (Fig. 3A). These results suggest that this interaction is direct and does not require additional proteins.

VASP is phosphorylated on Ser157, Ser239 and Thr278 in response to CXCL8 stimulation

Immunoblotting for VASP in CXCR2 immunoprecipitates revealed increased amounts of phosphorylated VASP present in immunoprecipitated samples from CXCL8-treated cells (Fig. 1B). It has previously been demonstrated that VASP is phosphorylated on Ser157 upon stimulation with the chemoattractant fMLP (Eckert and Jones, 2007). Western blot analysis on lysates from vehicle- and CXCL8-stimulated cells using a Ser157-*P* VASP-specific antibody confirmed that the shifted VASP band was Ser157-*P* VASP (Fig. 4A). Western blot analysis with a Ser239-*P* VASP-specific antibody confirmed that VASP was also phosphorylated on Ser239 in the EVH2 domain in response to CXCL8 (Fig. 4B). Some Ser239-*P* VASP is present in both molecular weight forms of VASP, indicating that some of the VASP is phosphorylated on both Ser157 and Ser239. Moreover, CXCL8 also induces VASP phosphorylation on Thr278, which is also present in both molecular weight forms of VASP (Fig. 4C).

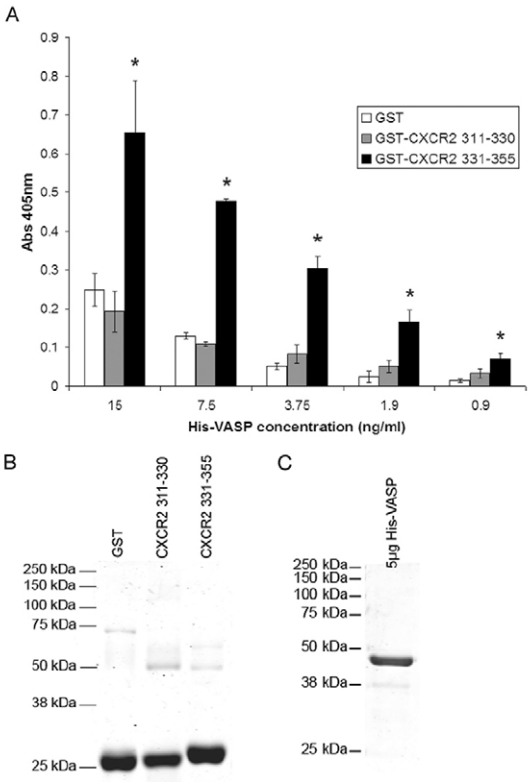

Fig. 3. Purified His_6-VASP interacts with amino acids 331-355 from the CXCR2 C-terminus. (A) 96-well plates were coated with 3 µg/ml GST, GST-CXCR2 311-330, or GST-CXCR2 331-355 and incubated with various concentrations of His_6-VASP (0.06-60 ng/ml). Bound His_6-VASP was detected using nickel-activated HRP (Abs 405 nm). Triplicate experiments show His_6-VASP binding (mean ± s.e.m.) to GST-CXCR2 331-355 was statistically higher than to GST alone or GST-CXCR2 311-330 (*$P \leq 0.05$, Mann Whitney U-test). Data shown are representative of at least three separate experiments. (B) Representative Coomassie-blue-stained gel of 5 µg purified GST, GST-CXCR2 311-330 and GST-CXCR2 331-355. (C) Representative Coomassie-blue-stained gel of 5 µg purified His_6-VASP.

To determine whether phosphorylation of VASP on Ser157 and Ser239 in response to CXCL8 was a specific CXCL8-mediated response or a general response to chemokine, cells were stimulated with CCL3 and examined for VASP phosphorylation (dHL60 cells endogenously express the CCR1 receptor for CCL3). Stimulation with CCL3 did not induce VASP phosphorylation on Ser157 (Fig. 4D), Ser239 (Fig. 4E) or Thr278 (Fig. 4F). These data suggest that VASP phosphorylation following chemokine stimulation is probably not a general response. Although treatment with CCL3 did not result in a VASP band shift, there was basal phosphorylation of Thr278 on VASP (Fig. 4F).

To determine which signaling pathways mediated the phosphorylation of VASP on Ser157, we analyzed CXCL8-stimulated cells incubated with a PKA inhibitor, H89 (20 µM), or the specific PKCδ inhibitor rottlerin (5 µM). These inhibitor concentrations are reasonably specific because the K_i of H89 for PKC is 31.7 µM and the IC_{50} of rottlerin for PKCα,β,γ is 30-42 µM.

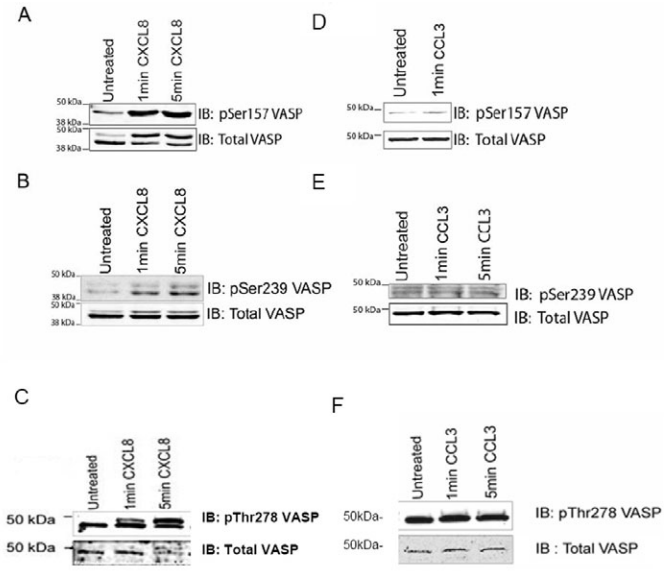

Fig. 4. VASP is phosphorylated on Ser157, Ser239 and Thr278 specifically in response to CXCL8 stimulation. HL-60-CXCR2 cells were stimulated with vehicle (Untreated) or 100 ng/ml CXCL8 for 1 or 5 minutes. Lysates were subjected to SDS-PAGE and western blot analysis (IB) using antibodies specific for Ser157-*P* (A), Ser239-*P* (B) or Thr278-*P* VASP (C). HL-60-CXCR2 cells were stimulated with vehicle (Untreated) or 100 ng/ml CCL3 for 1 minute. Lysates were subjected to SDS-PAGE and western blot analysis (IB) for Ser157-*P* (D), Ser239-*P* (E) or Thr278-*P* VASP (F). Data shown are representative of three separate experiments.

Both basal and CXCL8-induced VASP Ser157 phosphorylation were significantly inhibited by H89 treatment (Fig. 5A,B). Treatment of cells with rottlerin had no significant effect of CXCL8-induced VASP phosphorylation at Ser157 (Fig. 5C,D). There was no significant inhibition of CXCL8-induced VASP phosphorylation at Ser157 upon treatment with the broad classical PKC inhibitor Ro-32-0432 (data not shown). These data suggest that CXCL8 stimulation activates PKA-mediated signaling pathways, and that both basal and CXCL8-induced phosphorylation of VASP at Ser157 is largely mediated by PKA.

We also investigated the pathways that mediate the phosphorylation of VASP at Ser239 using the PKA inhibitor H89, the broad classical PKC inhibitor Ro-32-0432, and the specific PKCδ inhibitor rottlerin. No effect on basal or CXCL8-induced phosphorylation at Ser239 was observed with Ro-32-0432 treatment (data not shown). By contrast, CXCL8-induced phosphorylation of VASP on Ser239 was impaired at the 1 minute time point upon pretreatment with rottlerin (Fig. 5E,F) and with H89 (Fig. 5G,H) as indicated by a decrease in both molecular weight forms of VASP by western blot analysis using the Ser239-*P*-specific antibody. Since Ser239 is known to be preferentially phosphorylated by PKG, we also examined whether the PKG inhibitor KT5823 inhibited CXCL8-induced phosphorylation at this site; no inhibition was observed when cells were treated with this inhibitor (data not shown). These data suggest that CXCL8-induced phosphorylation of VASP on Ser239 occurs through both PKA- and PKCδ-dependent signaling pathways.

When CXCR2 was immunoprecipitated from HL-60 cells pretreated with rotterlin (5 μM), we observed that Rotterlin (5 μM) pretreatment greatly diminished the amount of Ser239-phosphorylated VASP in the lysate and the amount of Ser239-phosphorylated VASP that coimmunoprecipitated with CXCR2. Moreover, Rotterlin pretreatment eliminated the ligand-induced increase in the amount of total VASP present in the immunoprecipitate (supplementary material Fig. S1). By contrast, pretreatment of the CXCR2-expressing HL-60 cells with H-89 did not reduce the amount of total VASP immunoprecipitated with CXCR2 and only inhibited the amount of phosphorylation of VASP on Ser157 (supplementary material Fig. S2).

Phosphorylation of VASP in the EVH2 domain regulates its interaction with CXCR2

Double homozygous null VASP/Mena mouse embryonic fibroblasts that have only trace levels of EVL expression (MV^{D7} cells) (Bear et al., 2000) were transfected with vectors that allow expression of various GFP-tagged murine VASP serine and threonine mutants (Applewhite et al., 2007) to investigate the functional roles of phosphorylation in CXCR2 interaction. CXCR2-GST pull-down reactions were performed with lysates from MV^{D7} cells stably expressing GFP-tagged serine to alanine mutant murine VASP. As shown in Fig. 6A, mutation of both Ser235 and Thr274 (equivalent to human Ser239 and Thr278, respectively) to alanine resulted in decreased GST-CXCR2 C-terminus binding. Both of these residues are located within the EVH2 domain of VASP (Fig. 8A). Interestingly, mutation of either Ser235 or Thr274 in combination with the Ser153 to alanine mutation did not result in loss of binding to the GST-CXCR2 C-terminus. These data suggest that phosphorylation of either Ser235 or Thr274 of VASP enhances binding to CXCR2.

We next sought to determine whether phosphorylation of the purified EVH2 domain enhanced binding to CXCR2. Purified His_6-tagged VASP EVH2 domain was phosphorylated in vitro with the catalytic subunit of PKA and used in binding assays with GST-CXCR2 331-355. Incubation of His_6-VASP EVH2 domain with the PKA catalytic subunit resulted in robust phosphorylation on Ser235 as indicated by western blot with a phospho-specific antibody (Fig. 6B). Importantly, phosphorylation of the His_6-VASP EVH2 domain resulted in a significant increase in the binding of GST-CXCR2 331-355 (Fig. 6C). These data demonstrate that phosphorylation of residues in the VASP EVH2 domain enhances the interaction with CXCR2.

CXCR2 C-terminus preferentially interacts with VASP over Mena and EVL

Because the EVH1 and EVH2 domains of the three Ena/VASP family members are highly conserved, we investigated whether the CXCR2 interaction was specific for VASP or could occur with other family members. GST pull-down experiments were performed using the C-terminus of CXCR2 and lysates from MV^{D7} cells stably expressing GFP-VASP, GFP-Mena or GFP-EVL. CXCR2 pulled down GFP-VASP but very little GFP-EVL and no detectable GFP-Mena (Fig. 7). This suggests that CXCR2 preferentially interacts with a sequence specific for VASP.

CXCR2 interaction with VASP occurs through the VASP EVH2 domain and requires the coiled-coil region

To determine the region of VASP that is necessary for the CXCR2 interaction, a series of GST pull-down reactions using the C-terminus of CXCR2 were performed using lysates of MV^{D7} cells stably expressing GFP-EVH1 or GFP-EVH2 domains, and GFP-VASP in which the central proline-rich region was deleted. The

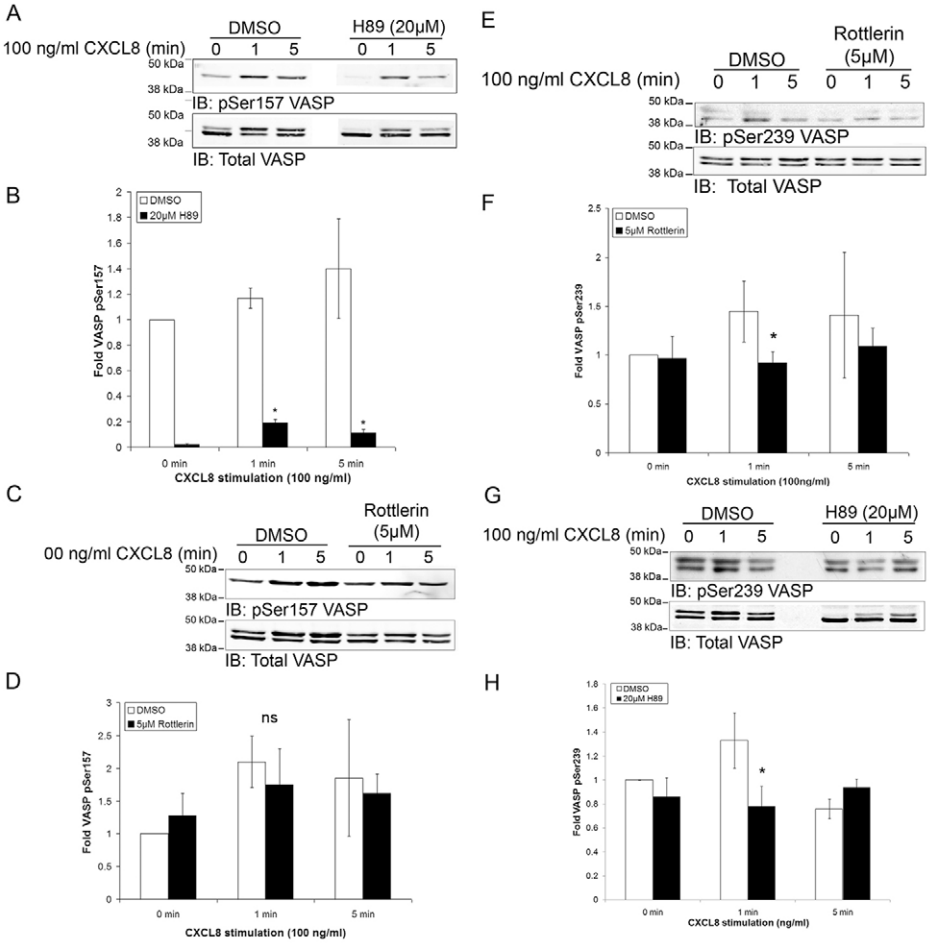

Fig. 5. Phosphorylation of VASP upon CXCL8 stimulation is mediated through PKA and PKC. Lysates from HL-60-CXCR2 cells pretreated with various inhibitors, stimulated with vehicle (0 minutes) or 100 ng /ml CXCL8 for 1 or 5 minutes and analyzed by SDS-PAGE and western blot. Statistical difference of mean ± s.e.m. in DMSO versus treatment is indicated (*$P \leq 0.05$, Mann Whitney U-test). (A) Cells pretreated with DMSO or 20 μM H89 for 60 minutes and analyzed by western blot using antibodies specific for VASP and VASP Ser157-*P*. (B) Quantification of normalized density of VASP Ser157-*P* in DMSO- versus H89-treated samples. (C) Cells pretreated with DMSO or 5 μM rottlerin for 15 minutes and analyzed by western blot analysis for VASP and VASP Ser157-*P*. (D) Quantification of normalized density of VASP Ser157-*P* in DMSO- versus rottlerin-treated samples. (E) Cells pretreated with DMSO or 5 μM rottlerin for 15 minutes and analyzed for VASP and VASP Ser239-*P* (F). Quantification of normalized density of VASP Ser239-*P* in DMSO- versus rottlerin-treated samples. (G) Cells pretreated with DMSO or 20 μM H89 for 60 minutes and analyzed using antibodies for VASP and VASP Ser239-*P*. (H) Quantification of normalized density of VASP Ser239-*P* in DMSO- versus H89-treated samples. Data shown represent average quantification from at least three separate experiments.

VASP GFP-EVH2 domain alone efficiently interacted with the GST C-terminus of CXCR2 in pull-down reactions (Fig. 8B). The EVH1 domain was not sufficient for binding and deletion of the proline-rich region of VASP did not interfere with binding, suggesting that these regions are not critical for the CXCR2 interaction.

To identify the precise region necessary for interaction with CXCR2, additional GST pull-down reactions were performed using lysates from MV^{D7} cells expressing GFP-VASP in which the F-actin binding (FAB) and tetramerization coiled-coil (COCO) regions were deleted. Deletion of the FAB region had no effect on GST-CXCR2 C-terminus binding (Fig. 8C). By contrast, deletion of the tetramerization COCO region completely eliminated the interaction with CXCR2 (Fig. 8C). It is also worth noting that GST pull-down reactions with lysates from MV^{D7} cells expressing a reverse coiled-coil (LH COCO) VASP mutant also revealed a binding deficiency (data not shown). These data suggest that either tetramerization of VASP creates the actual binding site for CXCR2 or that tetramerization maintains VASP in an orientation that is essential for the interaction with CXCR2.

F-actin is necessary for localization of VASP to the membrane and interaction with CXCR2

The phosphorylation of VASP on serine and threonine residues in the EVH2 domain interferes with its ability to interact with G- and F-actin (Barzik et al., 2005; Harbeck et al., 2000). In addition, we have shown that phosphorylation of VASP on Ser239 significantly enhances the VASP-CXCR2 interaction. These results suggested that CXCR2 and F-actin might be mutually exclusive in their binding to VASP. To investigate this hypothesis, we treated cells with 25 nM cytochalasin D (CD) to disrupt F-actin polymerization; low CD concentrations displace VASP from the leading edge, presumably by blocking barbed ends (Bear et al., 2002; Lacayo et al., 2007). We immunoprecipitated CXCR2 from the CD-treated cells and examined whether an increased amount of VASP was associated with CXCR2. Contrary to our expectations, CD treatment disrupted the CXCR2-VASP complex. Moreover, both the basal and the ligand induced coimmunoprecipitation of CXCR2 and VASP was reduced by CD treatment (Fig. 9A). It should be noted that the higher molecular weight form of VASP is predominantly detected in CXCR2 immunoprecipitates, indicative of the preferential association of phosphorylated VASP with CXCR2. Importantly, this disruption was not due to lack of VASP phosphorylation in response to CXCL8, because robust phosphorylation at Ser157 and Ser239 still occurred with CD treatment (Fig. 9B). These data indicate that F-actin is required for VASP binding to CXCR2 in cells.

As shown in the previous experiments, the CXCR2 C-terminus was used to test for interaction with the GFP-VASP-ΔFAB in pull-down assays and no defect in VASP-ΔFAB binding to GST-CXCR2 was observed (Fig. 8B). These data in combination suggest that the interaction of VASP with F-actin is necessary for proper VASP localization to the membrane and subsequent interaction with CXCR2. To test this hypothesis, we treated cells with 25 nM CD, stimulated directionally with CXCL8, and examined localization

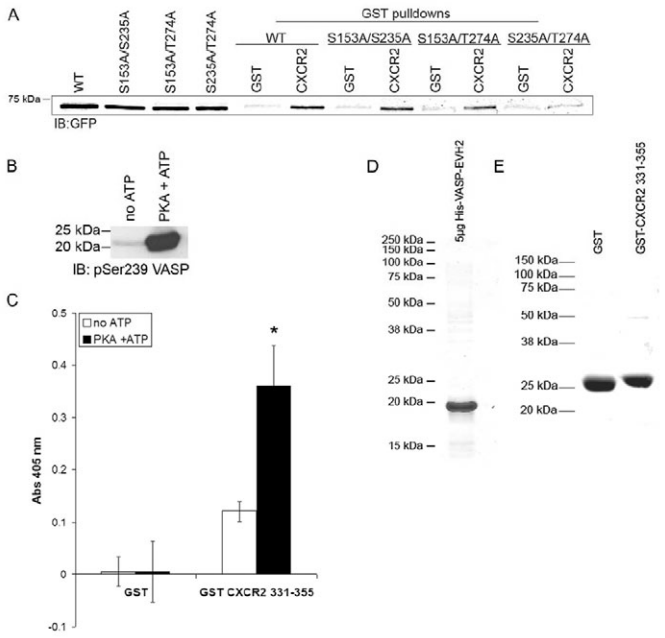

Fig. 6. Phosphorylation of VASP regulates its interaction with CXCR2. (A) Western blot analysis for GFP (IB) of GST pull-downs with GST or GST-CXCR2 C-terminus using lysates from MV^{D7} cells stably expressing GFP-VASP WT, S153A-S235A, S153-T274A and S235A-T274A. (B) Western blot analysis of purified His_6-VASP EVH2 domain incubated with catalytic subunit of PKA with and without ATP using a Ser235-*P*-specific antibody. (C) Binding (mean ± s.e.m.) of His_6-VASP EVH2 domain incubated with and without ATP to either GST or GST-CXCR2 331-355. Binding was detected by measuring absorbance at 405 nm from three separate experiments. Statistical significance of binding to GST-CXCR2 with or without ATP is indicated by $*P \leq 0.05$ (Mann Whitney U-test). (D) Representative Coomassie-blue-stained gel of 5 µg purified His_6-VASP EVH2. (E) Representative Coomassie-blue-stained gel of 5 µg of purified GST or GST-CXCR2 331-355.

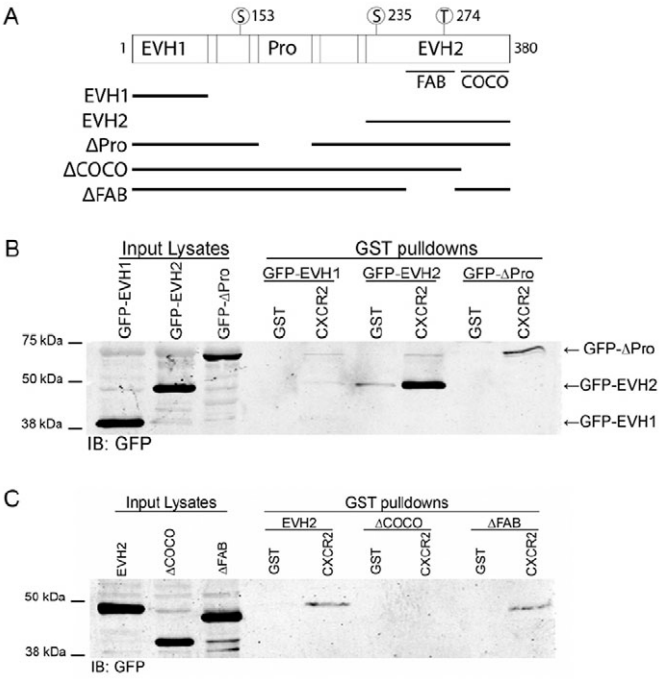

Fig. 8. CXCR2 interaction with VASP occurs through the VASP-EVH2 domain and requires the coiled-coil region. (A) Schematic of murine VASP domain structure and fragments used in pull-down experiments. Numbers indicate the amino acids phosphorylated in murine VASP. Western blot analysis for GFP (IB) to detect GFP-VASP of GST pull-downs with GST or GST-CXCR2 C-terminus using: (B) lysates from MV^{D7} cells stably expressing GFP-VASP-EVH1, GFP-VASP-EVH2 or GFP-VASP-ΔPro (deletion of proline-rich region) or (C) lysates from MV^{D7} cells stably expressing GFP-VASP-EVH2 WT, GFP-VASP-ΔCOCO (coiled-coil deletion), or GFP-VASP-ΔFAB (F-actin binding motif deletion). Data shown are representative of three separate experiments.

of VASP. Cells treated with CD exhibited largely cytoplasmic VASP distribution and diminished recruitment of VASP to the membrane with CXCR2 (Fig. 9C,D). The requirement for F-actin to properly localize VASP for interaction with CXCR2 was illustrated by loss of coimmunoprecipitation and decreased recruitment of VASP to the membrane with CD treatment. The reduction in coimmunoprecipitation of VASP and CXCR2, even in unstimulated cells treated with CD, supports the concept that VASP-actin association brings VASP to the membrane, where, upon ligand stimulation, phosphorylation of VASP and association of VASP with CXCR2 occur.

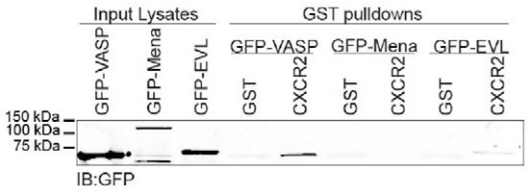

Fig. 7. CXCR2 preferentially interacts with VASP as opposed to Mena or EVL. Western blot analysis for GFP (IB) of GST pull-downs with GST or GST-CXCR2 C-terminus using lysates from MV^{D7} cells stably expressing GFP-VASP, GFP-Mena or GFP-EVL. Data shown are representative of three separate experiments.

VASP knockdown specifically impairs CXCR2-mediated chemotaxis

We next sought to determine the effects of knocking down expression of VASP on CXCR2-mediated chemotaxis. A reduction of VASP protein levels was observed in HL-60-CXCR2 cells stably expressing VASP shRNA compared with cells expressing non-silencing shRNA (Fig. 10A). Cells expressing VASP shRNA exhibited significantly impaired CXCR2-mediated chemotaxis when compared with cells expressing non-silencing shRNA (Fig. 10B). To determine whether the defect in chemotaxis was specific for CXCR2, we assessed CCL3-mediated chemotaxis in these cells and found that VASP knockdown did not impair CCL3-mediated chemotaxis (Fig. 10C). We also examined motility in response to global CXCL8 stimulation and observed a decrease in general chemokinesis but no difference in motility in the absence of CXCL8 (data not shown). In addition, there was no effect on adhesion of VASP-knockdown cells to fibronectin. Preliminary experiments examining peritoneal leukocyte recruitment in $VASP^{-/-}$ mice revealed deficiencies in CXCL8-mediated recruitment. These data indicate that VASP has a specific role in mediating CXCR2-mediated chemotaxis.

Cells expressing VASP shRNA exhibit impaired polarization in the direction of the CXCL8 gradient

The fact that cells expressing VASP shRNA exhibited normal CCR1-mediated chemotactic responses suggested that a defect

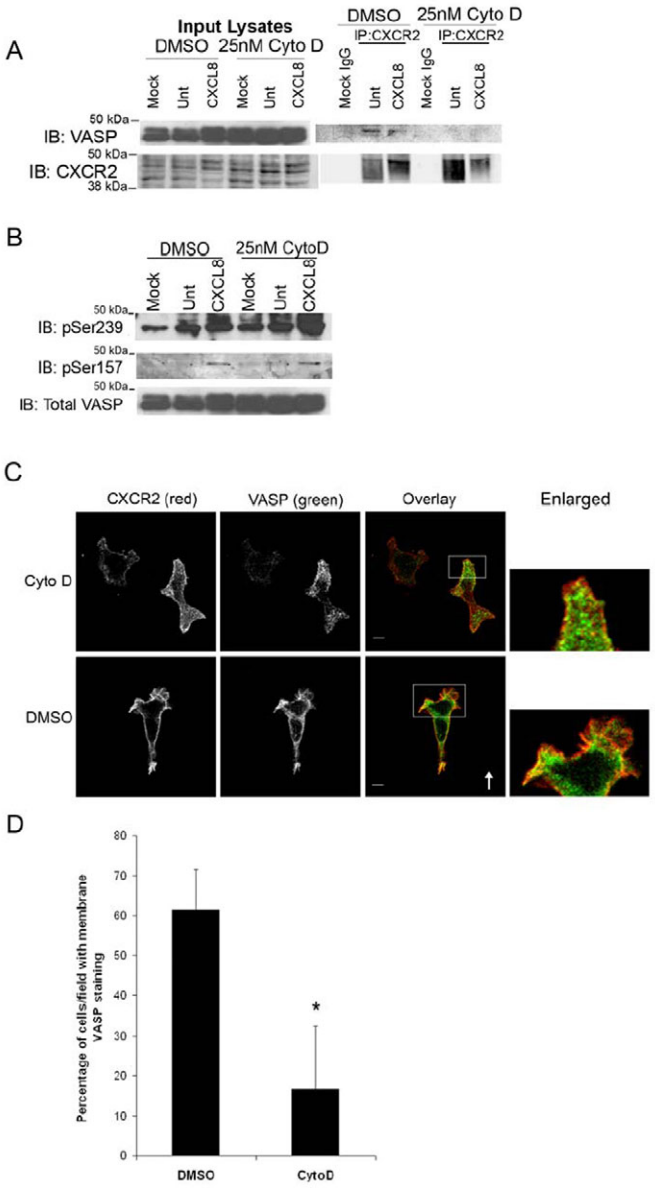

Fig. 9. F-actin is necessary for localization of VASP to the membrane and interaction with CXCR2. dHL-60 cells were pretreated for 30 minutes with 25 nM cytochalasin D (CytoD) or DMSO (vehicle), then stimulated with vehicle (Mock, Unt) or 100 ng/ml CXCL8 for 1 minute. (A) Cell lysates were incubated with either normal rabbit IgG (Mock IgG) or rabbit anti-CXCR2 antibody-coupled Sepharose. Eluted immunoprecipitated proteins were analyzed by SDS-PAGE and western blot (IB) for CXCR2 and VASP. (B) Western blot analysis (IB) using antibodies specific for VASP P-Ser157 or VASP Ser239-*P* of lysates. (C) Immunofluorescence confocal images of CXCR2, VASP and F-actin staining in dHL-60-CXCR2 cells and stimulated directionally with 50 ng/ml CXCL8 in Zigmond chamber for 15 minutes. The arrow indicates direction of CXCL8 gradient (0-50 ng/ml CXCL8). Image represents a single *z*-section of 0.49 µm. Enlarged panel images are magnified ×4 from original images. Overlay image is pseudocolored where green is VASP, red is CXCR2, and blue is F-Actin. Images were processed using Adobe Photoshop. Scale bars: 5 µm. (D) Quantification of mean ± s.e.m. percentage of cells per ×63 field exhibiting VASP immunofluorescence staining at the plasma membrane versus cytoplasm. Ten microscopic fields were examined for DMSO- and CytoD-treated cells with 2-8 cells per field Statistical significance of DMSO- versus CytoD-treated cells is indicated (**P*<0.0005, Student's *t*-test). Data shown are representative of three separate experiments.

in general motility was not the reason for deficient CXCL8-mediated chemotaxis. Therefore, we examined whether VASP-knockdown cells were able to polarize in the direction of CXCL8 gradients. These experiments revealed that cells expressing VASP shRNA exhibited significantly impaired directional polarization when compared with cells expressing non-silencing shRNA in response to CXCL8 gradients (Fig. 11A,C). Again, the specificity of this response was investigated by examining CCR1-mediated polarization of VASP-knockdown cells in response to CCL3 gradients. As shown in Fig. 11B,C, cells expressing VASP shRNA polarized efficiently toward CCL3 gradients. To

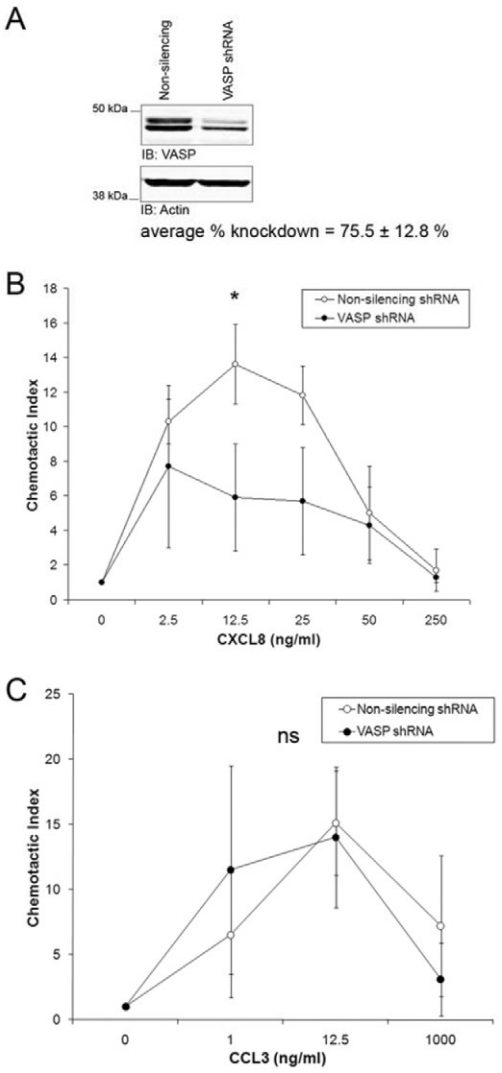

Fig. 10. Expression of VASP shRNA specifically impairs CXCR2-mediated chemotaxis. (A) Western blot analysis of VASP in lysates from HL-60-CXCR2 cells stably expressing non-silencing shRNA and VASP shRNA. Average percentage knockdown ± s.e.m. of VASP in western blots from three separate experiments. (B) Boyden chamber assay assessing chemotaxis of HL-60-CXCR2 cells stably expressing non-silencing or VASP shRNA in response to CXCL8 (B) or (C) in response to CCL3. Graphs represent the mean ± s.e.m. chemotactic index from three separate experiments. Statistical difference in dose response curve for CXCL8-mediated chemotaxis in non-silencing versus VASP shRNA expressing cells (**P*<0.01, one-way ANOVA). There was no significant difference (ns) in CCL3-mediated chemotaxis between non-silencing versus VASP shRNA expressing cells (one-way ANOVA).

investigate whether CXCL8-induced polarization deficiency resulted from the inability of the cells to adopt a polarized morphology or from a defect in the ability of the cells to respond to the CXCL8 gradient, the total number of cells polarized in any direction was examined with CXCL8 and CCL3 gradients. No difference was observed in the total number of polarized cells in response to either CXCL8 or CCL3 gradients upon VASP knockdown (Fig. 11D). These data imply that cells expressing

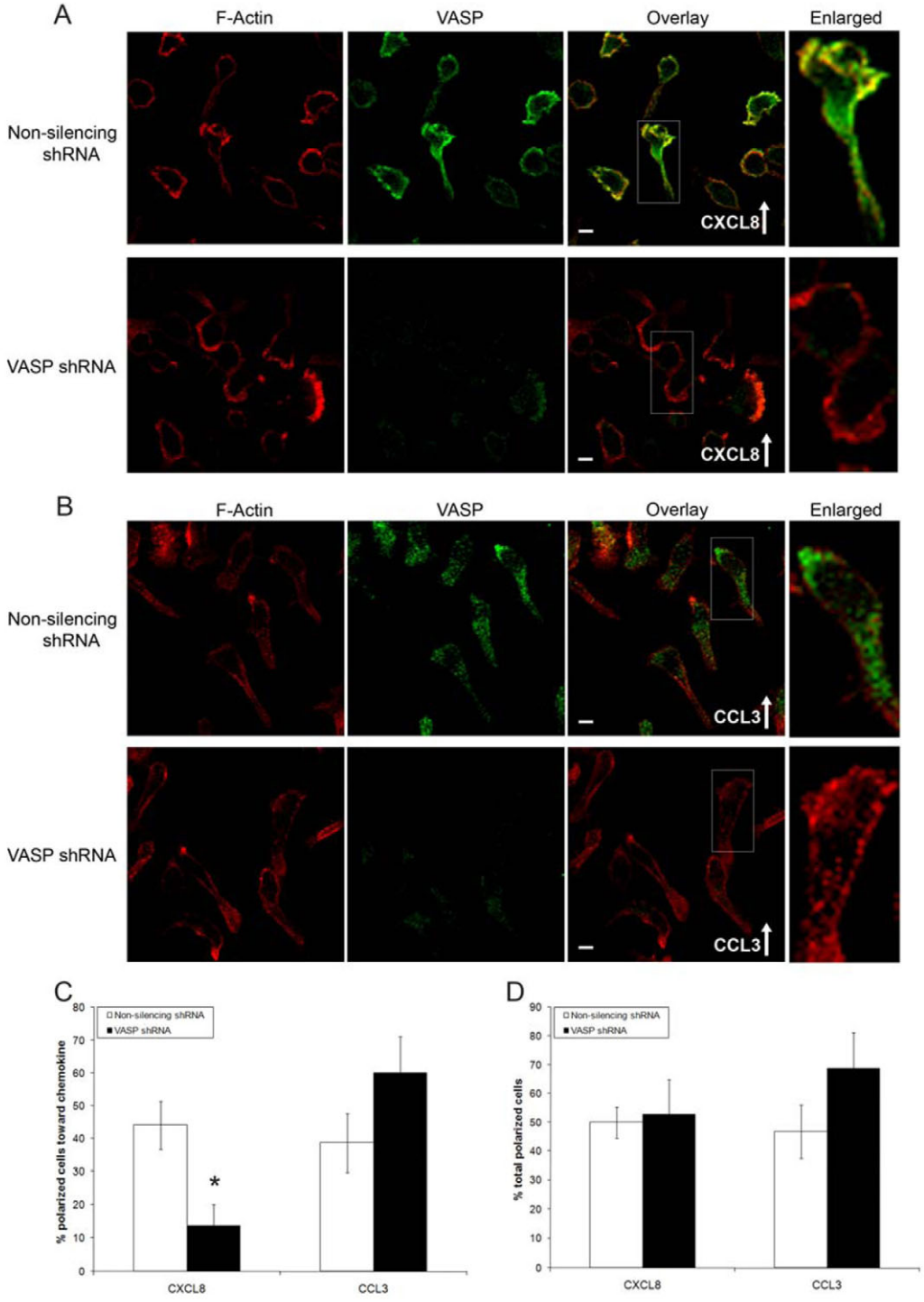

Fig. 11. Cells expressing VASP shRNA exhibit impaired CXCL8-induced cell polarization. Confocal images of cells expressing non-silencing or VASP shRNA stimulated directionally with 50 ng/ml of CXCL8 (A) or 50 ng/ml of CCL3 (B) in a Zigmond chamber for 15 minutes and stained using anti-VASP antibody (green) and phalloidin (red). Arrows indicate the direction of the gradients (0-50 ng/ml CXCL8 or CCL3). Enlarged panels are magnified ×2.5 original images. Scale bars: 5 μm (C). Quantification of mean ± s.e.m. number of cells per field polarized in the direction of the CXCL8 or CCL3 gradients. Statistical significance of non-silencing versus VASP shRNA is indicated (*P<0.001, Mann Whitney U-test). (D) Quantification of the mean ± s.e.m. number of polarized cells from images of 20 ×63 fields, each containing 25-50 cells. Data shown are representative of two separate experiments.

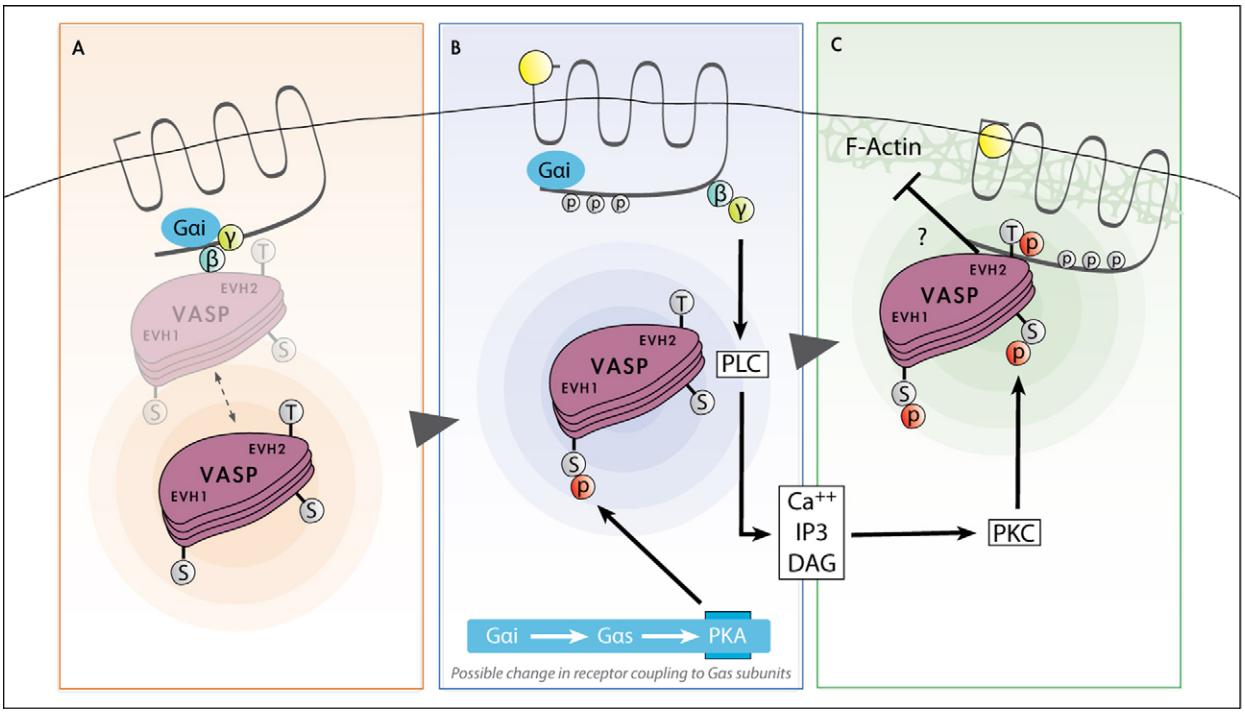

Fig. 12. Model illustrating the roles of VASP phosphorylation in mediating the VASP-CXCR2 interaction. (A) CXCR2 and VASP in unstimulated cells. VASP is predominantly located in the cytoplasm but might have some loose basal association with CXCR2. (B) Upon ligand binding, uncoupling of the G proteins occurs, activating PKA- and PKC-signaling pathways. VASP localizes to the plasma membrane. It is likely that there is a change in Gα coupling to CXCR2 to activate PKA, which phosphorylates VASP on Ser157 in the EVH1 domain. (C) Uncoupling of the Gβγ subunit activates PKC, which phosphorylates Ser239 and possibly Thr278 in the EVH2 domain of VASP. These phosphorylations allow strong interaction between VASP and CXCR2. CXCR2 binding to VASP is likely mutually exclusive with the F-Actin–VASP interaction but it is possible that when phosphorylated VASP is bound to CXCR2, sustained interaction with F-actin occurs.

VASP shRNA are able to exhibit a polarized morphology but specifically lack the ability to efficiently sense and polarize in response to the CXCL8 chemokine gradient.

Discussion

This study demonstrates an interaction between CXCR2 and VASP for the first time. VASP coimmunoprecipitates with CXCR2 and colocalization of VASP and CXCR2 is observed in both globally and directionally stimulated cells. A subpopulation of VASP colocalization with CXCR2 is seen in the lamellipodia of directionally stimulated cells, possibly representing phosphorylated VASP that interacts strongly with CXCR2. This CXCR2-VASP interaction might have an important role in the organization of the actin cytoskeleton in response to chemokines. In addition, the data show that leading edge VASP is phosphorylated on Ser239 through PKA- and probably PKCδ-mediated pathways, which enhances the interaction with CXCR2, suggesting that these signaling events are likely to have a key role in the chemotactic response.

Phosphorylation of VASP in the EVH2 domain reduces its G-actin and F-actin binding, and filament-bundling activity (Barzik et al., 2005; Harbeck et al., 2000). Therefore, it is of great interest that CXCL8 stimulation induces VASP phosphorylation on Ser239 and that this affects the binding of CXCR2 to VASP (Fig. 12). If binding of VASP to CXCR2 is mutually exclusive with F-actin interaction, this would represent a novel role for VASP in mediating the CXCR2-mediated chemotactic response. Alternatively, binding of phosphorylated VASP to CXCR2 might allow interaction with F-actin despite VASP phosphorylation in the EVH2 domain. Our data suggest that the CXCR2 interaction probably occurs through the COCO region, and phosphorylation in the EVH2 domain allows a favorable conformation for this interaction to occur. This same region of VASP was shown to be responsible for actin barbed-end capture (Pasic et al., 2008). Since VASP exists as a stable tetramer, it is also possible that tetramers of mixed phosphorylation status could bind both receptor and F-actin simultaneously.

Our data demonstrate that treatment of cells with low concentrations of CD ablates coimmunoprecipitation of VASP with CXCR2 and VASP localization to the membrane. This finding is consistent with previously published results illustrating displacement of Ena/VASP proteins from the leading edge upon low-dose CD treatment (Bear et al., 2002). Since the VASP mutant lacking the FAB motif (ΔFAB mutant) still binds the CXCR2 C-terminus, F-actin might be involved in proper localization of VASP, but might not be required for CXCR2 binding. Thus F-actin barbed ends are probably required for targeting of VASP to the membrane where the interaction with CXCR2 occurs.

Owing to its multidomain structure, VASP also has an important role as an adaptor molecule. VASP interacts with several focal adhesion and leading edge proteins through its EVH1 domain and a number of SH3-domain-containing proteins through its proline-rich region. The interaction of VASP with CXCR2 represents a direct link between the receptor and the actin cytoskeleton and might also serve as an adaptor linking CXCR2 to several additional potential mediators of chemotaxis.

All Ena/VASP family members share a common domain structure and can heterotetramerize via their EVH2 domains (Bachmann et al., 1999). Therefore, the observation that CXCR2 preferentially interacts with the EVH2 domain of VASP is surprising and suggests

a unique domain feature for this region in VASP. The Thr278 phosphorylation in the EVH2 domain is unique to VASP and little is known regarding the role of this unique site. Results from our experiments show that CXCL8 ligand induces VASP phosphorylation on Thr278, and this Thr278-phosphorylated VASP binds CXCR2. Moreover, lysates from MV^{D7} cells expressing VASP mutated at S235A and T274A lost CXCR2 binding. These data, and the fact that the CXCR2 interaction is preferential for VASP, suggest that phosphorylation at both EVH2 sites is important for the interaction. Very low levels of CXCR2 binding to EVL are not surprising because it lacks the serine phosphorylation site that we have shown enhances the interaction. Despite the presence of a phosphorylation site in the EVH2 domain of Mena, it fails to interact with CXCR2. These findings, together with our observation of impaired CXCR2-mediated chemotaxis and polarization in VASP-knockdown cells, argue for a unique function of VASP in CXCR2-mediated responses in leukocytes.

Unique roles for VASP in general motility have been identified previously in other cellular systems. For example, cardiac fibroblasts isolated from $VASP^{-/-}$ mice exhibit increased cell spreading, sustained Rac activation and decreased cell motility (Garcia Arguinzonis et al., 2002) and VASP knockdown in breast cancer cells revealed that VASP is crucial for migfilin-mediated migration (Zhang et al., 2006). VASP also has well-established roles in regulating platelet activation (Aszodi et al., 1999; Hauser et al., 1999; Pula et al., 2006). *Dictyostelium* Ddvasp-null cells exhibit less persistent chemotaxis and reduced directionality in response to a cAMP chemoattractant, suggesting defects in gradient sensing (Han et al., 2002).

Data presented here illustrate a direct connection between an activated CXCR2 chemokine receptor and VASP, linking polarization and gradient-sensing signals. This establishes a novel signaling role for VASP in translating the extracellular chemokine gradient to intracellular polarization cues. Since cells expressing VASP shRNA are still able to polarize in response to a CCL3 gradient but not a CXCL8 gradient, it appears that the polarization defect probably represents a deficiency in CXCR2-mediated CXCL8 gradient sensing. Alternatively, the CCL3 receptor might couple to another member of the VASP family to polarize the cell.

The proteomics approach used in this manuscript represents a valuable tool to identify components of the dynamic 'chemosynapse'. We propose that assembly of components at the cytoplasmic domains of activated chemokine receptors mediates signaling events and cytoskeletal reorganization necessary for chemokine receptor function. This approach was used to identify dynamic protein-protein interactions with CXCR2, and these studies have demonstrated for the first time that CXCR2 interacts with VASP. This interaction represents a direct link between CXCR2 and a regulator of the actin cytoskeleton and also potentially serves as a mechanism to link CXCR2 to other cellular signaling pathways involved in gradient sensing.

Materials and Methods

Materials and antibodies

Anti-CXCR2 affinity-purified polyclonal antibody was generated as described previously (Mueller et al., 1994). Normal rabbit IgG was obtained from Jackson ImmunoResearch (West Grove, PA). Anti-VASP polyclonal, anti-VASP phospho-serine 157, and anti-VASP phospho-serine 239 monoclonal antibodies were purchased from Calbiochem (San Diego, CA). Anti-GFP polyclonal antibody was from Abcam (Cambridge, MA). PKA inhibitor H-89, PKC inhibitor Ro-32-0432, and PKCδ inhibitor rottlerin were from Calbiochem (San Diego, CA). PKG inhibitor KT5823 was purchased from Sigma (St Louis, MO). Phosphate-buffered saline (PBS) was produced by dissolving 8 g NaCl, 0.2 g KCl, 1.44 g Na_2HPO_4 and 0.24 g KH_2PO_4 in 1 litre dH_2O and adjusting pH to 7.4. Bovine serum albumin (BSA) (Fraction V, ~99% purity, γ-globulin-free) was purchased from Sigma. Affinity-purified anti-phosphothreonine 278 rabbit peptide antibody (Blume et al., 2007) was a kind gift from Thomas Renne at Universitatsklinikum Wurzburg, Germany.

Plasmids, cell culture and transfection

Constructs for glutathione *S*-transferase (GST) fusion proteins of the C-terminal residues of CXCR2 (Fan et al., 2001b) and the HL-60 cell line expressing human CXCR2 have been previously described (Sai et al., 2006). HL-60 cells stably expressing non-silencing shRNA and VASP shRNA were generated using lentiviral infection. The pGIPZ-shRNAmir plasmids (Open Biosystems, Huntsville, AL) expressing non-silencing shRNA control sequence or VASP-specific shRNA sequence (5′-ccttgttctagattcacttta-3′) were packaged into lentiviral particles and CXCR2HL-60 cells were infected with the particles following the manufacturer's protocols. Stable cell lines were selected for resistance to puromycin (0.5 μg/ml) (Sigma). For all experiments, HL-60 cells were differentiated along the neutrophilic lineage (Servant et al., 1999). MV^{D7} cells were cultured as described previously (Bear et al., 2000).

CXCR2 immunoprecipitations and proteomics analyses

Purified normal rabbit IgG and anti-CXCR2 polyclonal antibodies were coupled to NHS-activated Sepharose beads (GE Healthcare, Piscataway, NJ). DHL-60 cells stably expressing CXCR2 were stimulated with vehicle (0.1% BSA-PBS) or 100 ng/ml CXCL8 for 1 minute and lysed in 50 mM Tris-HCl, pH 7.5, 0.05% Triton X-100, 300 mM NaCl, cleared by centrifugation, and precleared with normal rabbit IgG-coupled beads. Lysates were incubated with normal rabbit IgG-coupled (Mock) or anti-CXCR2 rabbit antibody-coupled beads. Proteins were eluted with Laemmli sample buffer, loaded onto a 10% polyacrylamide gel, stained with colloidal blue stain (Invitrogen, Carlsbad, CA) and bands subjected to in-gel trypsin digest. Tryptic peptides were analyzed by LC-MS/MS using a Thermo Finnigan LTQ ion trap mass spectrometer equipped with a Thermo MicroAS autosampler Thermo Surveyor HPLC pump, Nanospray source, and Xcalibur 1.4 instrument control. Analysis and protein identification procedures were described previously (Lapierre et al., 2007) with the exception that a human subset of the NCBI database downloaded in March 2005 and containing 124,917 entries was used for the Sequest searches. Unique proteins in each group were identified using the CHIPS (Complete Hierarchical Integration of Protein Searches) in-house database program. Only proteins identified in at least three of the four experiments by multiple peptides were analyzed further.

Western blot analysis

Proteins were separated by SDS-PAGE and transferred to nitrocellulose membrane (Bio-Rad Laboratories, Hercules, CA). Membranes were blocked with 5% nonfat milk in TBS buffer for 1 hour at room temperature, incubated with primary antibodies overnight at 4°C, and washed and incubated with species appropriate HRP-conjugated secondary antibodies diluted 1:10,000 (EMD Biosciences, San Diego, CA) or IRDye-conjugated secondary antibodies (Rockland Immunochemicals, Gilbertsville, PA and Invitrogen, Carlsbad, CA) diluted 1:20,000 for 1 hour at room temperature in the dark, and washed three times. Membranes were subjected to detection using ECL or scanned using Odyssey infrared imaging system (Licor Biosciences, Lincoln, NE) and FluorChem 8900 software (AlphaInnotech Corporation, San Leandro, CA).

Dephosphorylation of VASP by lambda phosphatase

Immunoprecipitates were incubated with 200 U of lambda phosphatase in lambda phosphatase buffer (50 mM Tris-HCl, 100 mM NaCl, 2 mM Dithiothreitol, 0.1 mM EGTA, 0.01% Brij 35) with 2 mM $MnCl_2$ at 30°C for 30 minutes, treated with sample buffer containing 5 mM DTT, and resolved on a 10% polyacrylamide-SDS gel.

Immunofluorescence staining and confocal microscopy

Cells in serum-free RPMI were seeded for 10 minutes at 37°C on glass coverslips coated with 100 μg/ml human fibronectin (BD Biosciences, San Diego, CA) and stimulated globally with vehicle (0.1% BSA/PBS) or 100 ng/ml CXCL8 diluted in 0.1% BSA-PBS at 37°C for indicated times or directionally with 50 ng/ml CXCL8 for 15 minutes using a Zigmond chamber (Neuroprobe, Gaithersburg, MD). Cells were fixed and processed for immunostaining as previously described (Neel et al., 2007). For phosphorylated VASP staining, cells were fixed 10 minutes in cytoskeletal buffer (10 mM N-morpholino ethanesulfonic acid (MES), pH 6.1, 3 mM $MgCl_2$, 0.138 M KCl, 2 mM EGTA) with 312.5 mM sucrose and 4% paraformaldehyde, permeabilized in cytoskeletal buffer with 312.5 mM sucrose and 0.5% Triton X-100 for 10 minutes, and blocked in 10% normal donkey serum (NDS) for 30 minutes. Primary anti-Ser157-*P* and anti-Ser239-*P* VASP antibodies were diluted in 0.5% NDS/PBS and incubated for 1 hour, washed three times with 0.5% NDS-PBS, incubated with fluorescence-conjugated secondary antibodies for 1 hour, washed three times, and mounted. Confocal images were acquired using a LSM-510 Meta laser-scanning microscope (Carl Zeiss, Thornwood, NY) with a ×63 1.3 NA oil-immersion lens and processed by Photoshop software (Adobe Systems, San Jose, CA).

Recombinant protein expression and purification

Recombinant His_6-tagged full length and EVH2 domain of VASP were purified from *Escherichia coli* as described previously (Barzik et al., 2005). Recombinant GST and

GST-CXCR2 C-terminus proteins were purified from *Escherichia coli* as described previously (Fan et al., 2002).

Direct binding of GST-CXCR2 331-355 and His_6-VASP

Proteins were isolated as described above and eluted with 50 mM Tris-HCl, pH 8.0, 10 mM reduced glutathione. 96-well polyvinyl plates were coated with 3 μg/ml GST or GST-CXCR2 331-355, blocked with 0.5% Tween20, 0.5% Triton X-100/PBS, and incubated with 15, 7.5, 3.25, 1.9 or 0.9 ng/μl His_6-VASP for 1 hour at room temperature. Plates were washed six times with 0.1% Tween20-PBS, incubated with 0.5 μg/ml His-Probe-HRP (Pierce, Milwaukee, WI), and washed six more times with 0.1% Tween20/PBS. Peroxidase substrate solution [50 mM sodium citrate buffer, pH 4.2, 90 mM 2,2′-azino-bis (3-ethylbenzothiazoline-6-sulfonic acid) (ABTS) (Sigma), 0.05 mM H_2O_2] was added to each well. Reactions were terminated with an equal volume of 1% SDS (Sigma) (w/v) solution. Substrate color intensities were measured at 405 nm using an $ELX800_{NB}$ plate reader (Bio-Tek Instruments, Winooski, VT). Assays were performed in triplicate.

Phosphorylation of His_6-VASP EVH2 with PKA

The His_6-VASP EVH2 domain was purified from *Escherichia coli* and protein was concentrated using Amicon Ultracentrifugal filter devices (MWCO 5000 Da) (Millipore, Billerica, MA). 50 μg purified His_6-VASP EVH2 was incubated with 2500 U cAMP-dependent protein kinase A (PKA) catalytic subunit (New England Biolabs, Ipswich, MA) with 100 mM ATP for 30 minutes at 30°C.

GST pull-down reactions from MV^{D7} cell lysates

MV^{D7} cells were lysed in 50 mM Tris-HCl pH 7.5, 0.05% Triton X-100, 300 mM NaCl containing mammalian protease inhibitor cocktail and phosphatase inhibitor cocktails I and II (Sigma). Lysates were cleared by centrifugation and incubated with 50 μg GST or GST-CXCR2 C-terminus coupled to glutathione agarose for 1 hour at 4°C. Agarose was washed three times with lysis buffer, proteins were eluted with 2× Laemmli sample buffer, and subjected to SDS-PAGE western blot analysis.

Chemotaxis and chemokinesis assays in a modified Boyden chamber

Chemotaxis assays were performed as previously described (Sai et al., 2008) with dHL-60 cells stably expressing CXCR2 and either non-silencing or VASP shRNA plasmids. The indicated concentrations of CXCL8 and murine CCL3 (Peprotech, Rocky Hill, NJ) were prepared in 1% BSA-phenol-red-free RPMI (chemotaxis buffer) and loaded into 96-well plate in duplicate. Chemokinesis experiments were performed as described by Sai et al. (Sai et al., 2008).

Quantification of cell polarization in Zigmond Chamber

dHL-60 cells stably expressing CXCR2 and either non-silencing or VASP shRNA were seeded and stimulated in a Zigmond chamber, using protocols described by Sai et al. (Sai et al., 2008). After fixation, cells were stained with phalloidin (Invitrogen, Carlsbad, CA) and VASP polyclonal rabbit antibody. Confocal images of 20 randomly selected ×63 microscopic fields were collected for each treatment and cell line. Approximately 25-50 cells were in each microscopic field. Cells elongated in the direction of the chemokine gradient and with polarized F-actin in the direction of the gradient were counted. This number was divided by the total number of cells present in the field to obtain the percentage of polarized cells.

Statistical analysis

Statistically significant differences between two groups were determined using the nonparametric two-tailed Mann Whitney U-test (Wilcoxin rank-sum test). One-way ANOVA analysis followed by a Bonferroni post test was used to determine statistically significant differences between more than two groups. All statistical analysis was performed using GraphPad Prism 5 software (GraphPad Software, San Diego, CA).

We are indebted to Sam Wells, Dawn Kilkenny, and the VUMC Cell Imaging Shared Resource for help with confocal images (NIH grants DK-20593, DK-58404, HD-15052, DK-59637 and EY-08126). We thank David Blum for his assistance in assay development, Thomas Renne for the Thr278 phospho-VASP antibody, and Elaine M. Pinheiro (M.I.T.) for assistance with animal studies. This work was supported by grants CA-34590 (to A.R.) and GM-58801 (to F.B.G.) and 1U54 CA112967-03 (to F.B.G.), T32CA09592 (to N.F.N.) and CA68485 from the NIH, and a Career Scientist Award from the Department of Veterans Affairs (to A.R.). Deposited in PMC for release after 12 months.

References

Applewhite, D. A., Barzik, M., Kojima, S., Svitkina, T. M., Gertler, F. B. and Borisy, G. G. (2007). Ena/VASP proteins have an anti-capping independent function in filopodia formation. *Mol. Biol. Cell* **18**, 2579-2591.

Aszodi, A., Pfeifer, A., Ahmad, M., Glauner, M., Zhou, X. H., Ny, L., Andersson, K. E., Kehrel, B., Offermanns, S. and Fassler, R. (1999). The vasodilator-stimulated phosphoprotein (VASP) is involved in cGMP- and cAMP-mediated inhibition of agonist-induced platelet aggregation, but is dispensable for smooth muscle function. *EMBO J.* **18**, 37-48.

Bachmann, C., Fischer, L., Walter, U. and Reinhard, M. (1999). The EVH2 domain of the vasodilator-stimulated phosphoprotein mediates tetramerization, F-actin binding, and actin bundle formation. *J. Biol. Chem.* **274**, 23549-23557.

Barzik, M., Kotova, T. I., Higgs, H. N., Hazelwood, L., Hanein, D., Gertler, F. B. and Schafer, D. A. (2005). Ena/VASP proteins enhance actin polymerization in the presence of barbed end capping proteins. *J. Biol. Chem.* **280**, 28653-28662.

Bashaw, G. J., Kidd, T., Murray, D., Pawson, T. and Goodman, C. S. (2000). Repulsive axon guidance: Abelson and Enabled play opposing roles downstream of the roundabout receptor. *Cell* **101**, 703-715.

Bear, J. E., Loureiro, J. J., Libova, I., Fassler, R., Wehland, J. and Gertler, F. B. (2000). Negative regulation of fibroblast motility by Ena/VASP proteins. *Cell* **101**, 717-728.

Bear, J. E., Svitkina, T. M., Krause, M., Schafer, D. A., Loureiro, J. J., Strasser, G. A., Maly, I. V., Chaga, O. Y., Cooper, J. A., Borisy, G. G. et al. (2002). Antagonism between Ena/VASP proteins and actin filament capping regulates fibroblast motility. *Cell* **109**, 509-521.

Benz, P. M., Blume, C., Moebius, J., Oschatz, C., Schuh, K., Sickmann, A., Walter, U., Feller, S. M. and Renné, T. (2008). Cytoskeleton assembly at endothelial cell-cell contacts is regulated by alphaII-spectrin-VASP complexes. *J. Cell Biol.* **180**, 205-219.

Blume, C., Benz, P. M., Walter, U., Ha, J., Kemp, B. E. and Renne, T. (2007). AMP-activated protein kinase impairs endothelial actin cytoskeleton assembly by phosphorylating vasodilator-stimulated phosphoprotein. *J. Biol. Chem.* **282**, 4601-4612.

Butt, E., Abel, K., Krieger, M., Palm, D., Hoppe, V., Hoppe, J. and Walter, U. (1994). cAMP- and cGMP-dependent protein kinase phosphorylation sites of the focal adhesion vasodilator-stimulated phosphoprotein (VASP) in vitro and in intact human platelets. *J. Biol. Chem.* **269**, 14509-14517.

Chitaley, K., Chen, L., Galler, A., Walter, U., Daum, G. and Clowes, A. W. (2004). Vasodilator-stimulated phosphoprotein is a substrate for protein kinase C. *FEBS Lett.* **556**, 211-215.

Eckert, R. E. and Jones, S. L. (2007). Regulation of VASP serine 157 phosphorylation in human neutrophils after stimulation by a chemoattractant. *J. Leukoc. Biol.* **82**, 1311-1321.

Eigenthaler, M., Nolte, C., Halbrugge, M. and Walter, U. (1992). Concentration and regulation of cyclic nucleotides, cyclic-nucleotide-dependent protein kinases and one of their major substrates in human platelets: estimating the rate of cAMP-regulated and cGMP-regulated protein phosphorylation in intact cells. *Eur. J. Biochem.* **205**, 471-481.

Fan, G. H., Yang, W., Sai, J. and Richmond, A. (2001a). Phosphorylation-independent association of CXCR2 with the protein phosphatase 2A core enzyme. *J. Biol. Chem.* **276**, 16960-16968.

Fan, G. H., Yang, W., Wang, X. J., Qian, Q. and Richmond, A. (2001b). Identification of a motif in the carboxyl terminus of CXCR2 that is involved in adaptin 2 binding and receptor internalization. *Biochemistry* **40**, 791-800.

Fan, G. H., Yang, W., Sai, J. and Richmond, A. (2002). Hsc/Hsp70 interacting protein (hip) associates with CXCR2 and regulates the receptor signaling and trafficking. *J. Biol. Chem.* **277**, 6590-6597.

Ferron, F., Rebowski, G., Lee, S. H. and Dominguez, R. (2007). Structural basis for the recruitment of profilin-actin complexes during filament elongation by Ena/VASP. *EMBO J.* **26**, 4597-4606.

Garcia Arguinzonis, M. I., Galler, A. B., Walter, U., Reinhard, M. and Simm, A. (2002). Increased spreading, Rac/p21-activated kinase (PAK) activity, and compromised cell motility in cells deficient in vasodilator-stimulated phosphoprotein (VASP). *J. Biol. Chem.* **277**, 45604-45610.

Gertler, F. B., Niebuhr, K., Reinhard, M., Wehland, J. and Soriano, P. (1996). Mena, a relative of VASP and Drosophila Enabled, is implicated in the control of microfilament dynamics. *Cell* **87**, 227-239.

Halbrugge, M., Friedrich, C., Eigenthaler, M., Schanzenbacher, P. and Walter, U. (1990). Stoichiometric and reversible phosphorylation of a 46-kDa protein in human platelets in response to cGMP- and cAMP-elevating vasodilators. *J. Biol. Chem.* **265**, 3088-3093.

Han, Y. H., Chung, C. Y., Wessels, D., Stephens, S., Titus, M. A., Soll, D. R. and Firtel, R. A. (2002). Requirement of a vasodilator-stimulated phosphoprotein family member for cell adhesion, the formation of filopodia, and chemotaxis in dictyostelium. *J. Biol. Chem.* **277**, 49877-49887.

Harbeck, B., Huttelmaier, S., Schluter, K., Jockusch, B. M. and Illenberger, S. (2000). Phosphorylation of the vasodilator-stimulated phosphoprotein regulates its interaction with actin. *J. Biol. Chem.* **275**, 30817-30825.

Hauser, W., Knobeloch, K. P., Eigenthaler, M., Gambaryan, S., Krenn, V., Geiger, J., Glazova, M., Rohde, E., Horak, I., Walter, U. et al. (1999). Megakaryocyte hyperplasia and enhanced agonist-induced platelet activation in vasodilator-stimulated phosphoprotein knockout mice. *Proc. Natl. Acad. Sci. USA* **96**, 8120-8125.

Jones, S. A., Moser, B. and Thelen, M. (1995). A comparison of post-receptor signal transduction events in Jurkat cells transfected with either IL-8R1 or IL-8R2. Chemokine mediated activation of p42/p44 MAP-kinase (ERK-2). *FEBS Lett.* **364**, 211-214.

Krause, M., Dent, E. W., Bear, J. E., Loureiro, J. J. and Gertler, F. B. (2003). Ena/VASP proteins: regulators of the actin cytoskeleton and cell migration. *Annu. Rev. Cell Dev. Biol.* **19**, 541-564.

Kwiatkowski, A. V., Rubinson, D. A., Dent, E. W., Edward van Veen, J., Leslie, J. D., Zhang, J., Mebane, L. M., Philippar, U., Pinheiro, E. M., Burds, A. A. et al. (2007). Ena/VASP Is Required for neuritogenesis in the developing cortex. *Neuron* **56**, 441-455.

Lacayo, C. I., Pincus, Z., VanDuijn, M. M., Wilson, C. A., Fletcher, D. A., Gertler, F. B., Mogilner, A. and Theriot, J. A. (2007). Emergence of large-scale cell morphology and movement from local actin filament growth dynamics. *PLoS Biol.* **5**, e233.

Lambrechts, A., Kwiatkowski, A. V., Lanier, L. M., Bear, J. E., Vandekerckhove, J., Ampe, C. and Gertler, F. B. (2000). cAMP-dependent protein kinase phosphorylation of EVL, a Mena/VASP relative, regulates its interaction with actin and SH3 domains. *J. Biol. Chem.* **275**, 36143-36151.

Lanier, L. M., Gates, M. A., Witke, W., Menzies, A. S., Wehman, A. M., Macklis, J. D., Kwiatkowski, D., Soriano, P. and Gertler, F. B. (1999). Mena is required for neurulation and commissure formation. *Neuron* **22**, 313-325.

Lapierre, L. A., Avant, K. M., Caldwell, C. M., Ham, A. J., Hill, S., Williams, J. A., Smolka, A. J. and Goldenring, J. R. (2007). Characterization of immunoisolated human gastric parietal cells tubulovesicles: identification of regulators of apical recycling. *Am. J. Physiol. Gastrointest. Liver Physiol.* **292**, G1249-G1262.

Lindsay, S. L., Ramsey, S., Aitchison, M., Renne, T. and Evans, T. J. (2007). Modulation of lamellipodial structure and dynamics by NO-dependent phosphorylation of VASP Ser239. *J. Cell Sci.* **120**, 3011-3021.

Loureiro, J. J., Rubinson, D. A., Bear, J. E., Baltus, G. A., Kwiatkowski, A. V. and Gertler, F. B. (2002). Critical roles of phosphorylation and actin binding motifs, but not the central proline-rich region, for Ena/vasodilator-stimulated phosphoprotein (VASP) function during cell migration. *Mol. Biol. Cell* **13**, 2533-2546.

Luttrell, L. M., Daaka, Y. and Lefkowitz, R. J. (1999). Regulation of tyrosine kinase cascades by G-protein-coupled receptors. *Curr. Opin. Cell Biol.* **11**, 177-183.

Menzies, A. S., Aszodi, A., Williams, S. E., Pfeifer, A., Wehman, A. M., Goh, K. L., Mason, C. A., Fassler, R. and Gertler, F. B. (2004). Mena and vasodilator-stimulated phosphoprotein are required for multiple actin-dependent processes that shape the vertebrate nervous system. *J. Neurosci.* **24**, 8029-8038.

Mueller, S. G., Schraw, W. P. and Richmond, A. (1994). Melanoma growth stimulatory activity enhances the phosphorylation of the class II interleukin-8 receptor in non-hematopoietic cells. *J. Biol. Chem.* **269**, 1973-1980.

Neel, N. F., Lapierre, L. A., Goldenring, J. R. and Richmond, A. (2007). RhoB plays an essential role in CXCR2 sorting decisions. *J. Cell Sci.* **120**, 1559-1571.

Neptune, E. R., Iiri, T. and Bourne, H. R. (1999). Galphai is not required for chemotaxis mediated by Gi-coupled receptors. *J. Biol. Chem.* **274**, 2824-2828.

Pasic, L., Kotova, T. and Schafer, D. A. (2008). Ena/VASP proteins capture actin filament barbed ends. *J. Biol. Chem.* **283**, 9814-9819.

Pula, G., Schuh, K., Nakayama, K., Nakayama, K. I., Walter, U. and Poole, A. W. (2006). PKCdelta regulates collagen-induced platelet aggregation through inhibition of VASP-mediated filopodia formation. *Blood* **108**, 4035-4044.

Reinhard, M., Halbrugge, M., Scheer, U., Wiegand, C., Jockusch, B. M. and Walter, U. (1992). The 46/50 kDa phosphoprotein VASP purified from human platelets is a novel protein associated with actin filaments and focal contacts. *EMBO J.* **11**, 2063-2070.

Richardson, R. M., Pridgen, B. C., Haribabu, B., Ali, H. and Snyderman, R. (1998). Differential cross-regulation of the human chemokine receptors CXCR1 and CXCR2. Evidence for time-dependent signal generation. *J. Biol. Chem.* **273**, 23830-23836.

Sai, J., Walker, G., Wikswo, J. and Richmond, A. (2006). The IL sequence in the LLKI motif in CXCR2 is required for full lligand-induced activation of Erk, Akt, and chemotaxis in HL-60 cells. *J. Biol. Chem.* **281**, 35931-35941.

Sai, J., Raman, D., Liu, Y., Wikswo, J. and Richmond, A. (2008). Parallel PI3K-dependent and src-independent pathways lead to CXCL8-mediated Rac2 activation and chemotaxis. *J. Biol. Chem.* **283**, 26538-26547.

Servant, G., Weiner, O. D., Neptune, E. R., Sedat, J. W. and Bourne H. R. (1999). Dynamics of a chemoattractant receptor in living neutrophils during chemotaxis. *Mol. Bio. Cell* **10**, 1163-1178.

Skoble, J., Auerbuch, V., Goley, E. D., Welch, M. D. and Portnoy, D. A. (2001). Pivotal role of VASP in Arp2/3 complex-mediated actin nucleation, actin branch-formation, and Listeria monocytogenes motility. *J. Cell Biol.* **155**, 89-100.

Tilton, B., Ho, L., Oberlin, E., Loetscher, P., Baleux, F., Clark-Lewis, I. and Thelen, M. (2000). Signal transduction by CXC chemokine receptor 4. Stromal cell-derived factor 1 stimulates prolonged protein kinase B and extracellular signal-regulated kinase 2 activation in T lymphocytes. *J. Exp. Med.* **192**, 313-324.

Wills, Z., Bateman, J., Korey, C. A., Comer, A. and Van Vactor, D. (1999). The tyrosine kinase Abl and its substrate enabled collaborate with the receptor phosphatase Dlar to control motor axon guidance. *Neuron* **22**, 301-312.

Zhang, Y., Tu, Y., Gkretsi, V. and Wu, C. (2006). Migfilin interacts with vasodilator-stimulated phosphoprotein (VASP) and regulates VASP localization to cell-matrix adhesions and migration. *J. Biol. Chem.* **281**, 12397-12407.